Proapoptotic Rassf1A/Mst1 signaling in cardiac fibroblasts is protective against pressure overload in mice

Dominic P. Del Re,[1] Takahisa Matsuda,[1] Peiyong Zhai,[1] Shumin Gao,[1] Geoffrey J. Clark,[2] Louise Van Der Weyden,[3] and Junichi Sadoshima[1]

[1]Department of Cell Biology and Molecular Medicine, Cardiovascular Research Institute, New Jersey Medical School, University of Medicine and Dentistry of New Jersey, Newark, New Jersey, USA. [2]Molecular Targets Group, J.G. Brown Cancer Center, University of Louisville, Louisville, Kentucky, USA. [3]Experimental Cancer Genetics, Wellcome Trust Sanger Institute, Wellcome Trust Genome Campus, Hinxton, Cambridge, United Kingdom.

Mammalian sterile 20-like kinase 1 (Mst1) is a mammalian homolog of *Drosophila* Hippo, the master regulator of cell death, proliferation, and organ size in flies. It is the chief component of the mammalian Hippo pathway and promotes apoptosis and inhibits compensatory cardiac hypertrophy, playing a critical role in mediating heart failure. How Mst1 is regulated, however, remains unclear. Using genetically altered mice in which expression of the tumor suppressor Ras-association domain family 1 isoform A (Rassf1A) was modulated in a cell type–specific manner, we demonstrate here that Rassf1A is an endogenous activator of Mst1 in the heart. Although the Rassf1A/Mst1 pathway promoted apoptosis in cardiomyocytes, thereby playing a detrimental role, the same pathway surprisingly inhibited fibroblast proliferation and cardiac hypertrophy through both cell-autonomous and autocrine/paracrine mechanisms, playing a protective role during pressure overload. In cardiac fibroblasts, the Rassf1A/Mst1 pathway negatively regulated TNF-α, a key mediator of hypertrophy, fibrosis, and resulting cardiac dysfunction. These results suggest that the functional consequence of activating the proapoptotic Rassf1A/Mst1 pathway during pressure overload is cell type dependent in the heart and that suppressing this mechanism in cardiac fibroblasts could be detrimental.

Introduction

Mammalian sterile 20-like kinase 1 (Mst1) is a ubiquitously expressed serine/threonine kinase and an important regulator of cell growth, proliferation, and apoptosis. It is evolutionarily conserved from flies to mammals and is a mammalian homolog of *Drosophila* Hippo (1), the master regulator of cell death, proliferation, and organ size in flies. Mst1 is activated by genotoxic compounds and cellular stress as well as in models of heart disease, including ischemia/reperfusion (I/R) injury and myocardial infarction (MI) (2, 3). Prior work from our lab has demonstrated the importance of Mst1 in modulating cardiac hypertrophy and apoptosis, ultimately affecting heart function, and identified Mst1 as a potential target of intervention in heart failure (2, 3). For example, Mst1 induces cardiomyocyte apoptosis, which plays an important role in mediating cardiac injury caused by I/R and progression of cardiac dysfunction after chronic MI. Mst1 also regulates heart size by activating its downstream kinase, Lats2, thereby inhibiting compensatory cardiomyocyte growth (4). The lack of compensatory hypertrophy induces increased wall stress and consequent myocardial cell death. It has been shown that Mst1 is activated by either phosphorylation or caspase-mediated cleavage. Importantly, however, the regulation of Mst1 activity in the heart has yet to be elucidated and will be critically important in our understanding of the progression of heart disease.

The Ras-association domain family (Rassf) proteins are a family of polypeptides initially discovered as Ras-GTP binding proteins and soon thereafter described as products of tumor suppressor genes (5–8). Rassf1 isoform A (Rassf1A) exhibits loss of heterozygosity in several lung cancers and is silenced through CpG promoter methylation in a wide range of tumor types (9, 10). Additionally, deletion of *rassf1A* leads to increased tumorigenesis in aged mice (11, 12). Rassf1A, like all members of the Rassf family, contains both a Ras association (RA) domain and a Salvador/Rassf/Hippo (SARAH) domain located at its carboxyl terminus (13, 14). The RA domain enables binding to activated Ras proteins (9, 15, 16), whereas the SARAH domain allows for interaction with Mst1/2 (17, 18). Because of its noncatalytic nature, Rassf1A is thought to serve an adapter function, acting as a scaffold to localize signaling in the cell.

Although previous studies conducted in vitro with overexpression systems have shown that Rassf1A and its closely related family member novel Ras effector 1 (NORE1; also referred to as Rassf5) can associate with Mst1, whether these proteins act as physiological regulators of Mst1 activation remains to be elucidated (17, 19–21). Furthermore, the *Drosophila* homolog, dRASSF, was shown to strongly associate with Hippo but antagonized its activation in the fly (22), leaving the mechanism of Mst1/Hippo regulation unresolved. In light of these discrepancies, our initial goals were to determine whether endogenous Rassf1A is a physiological regulator of Mst1 in the heart in vivo and to evaluate the functional significance of the Rassf1A/Mst1 pathway in the heart under stress.

The findings of our present study establish Rassf1A as a physiological activator of Mst1 in the mammalian heart. Unexpectedly, we found that the function of the Rassf1A/Mst1 pathway was quite different between cardiomyocytes and fibroblasts: Rassf1A/Mst1 primarily stimulated apoptosis in cardiomyocytes, whereas it primarily inhibited cell proliferation in cardiac fibroblasts. Furthermore, suppression of the Rassf1A/Mst1 pathway in cardiomyocytes was salutary through suppression of apoptosis, whereas inhibition

Conflict of interest: The authors have declared that no conflict of interest exists.
Citation for this article: *J Clin Invest.* 2010;120(10):3555–3567. doi:10.1172/JCI43569.

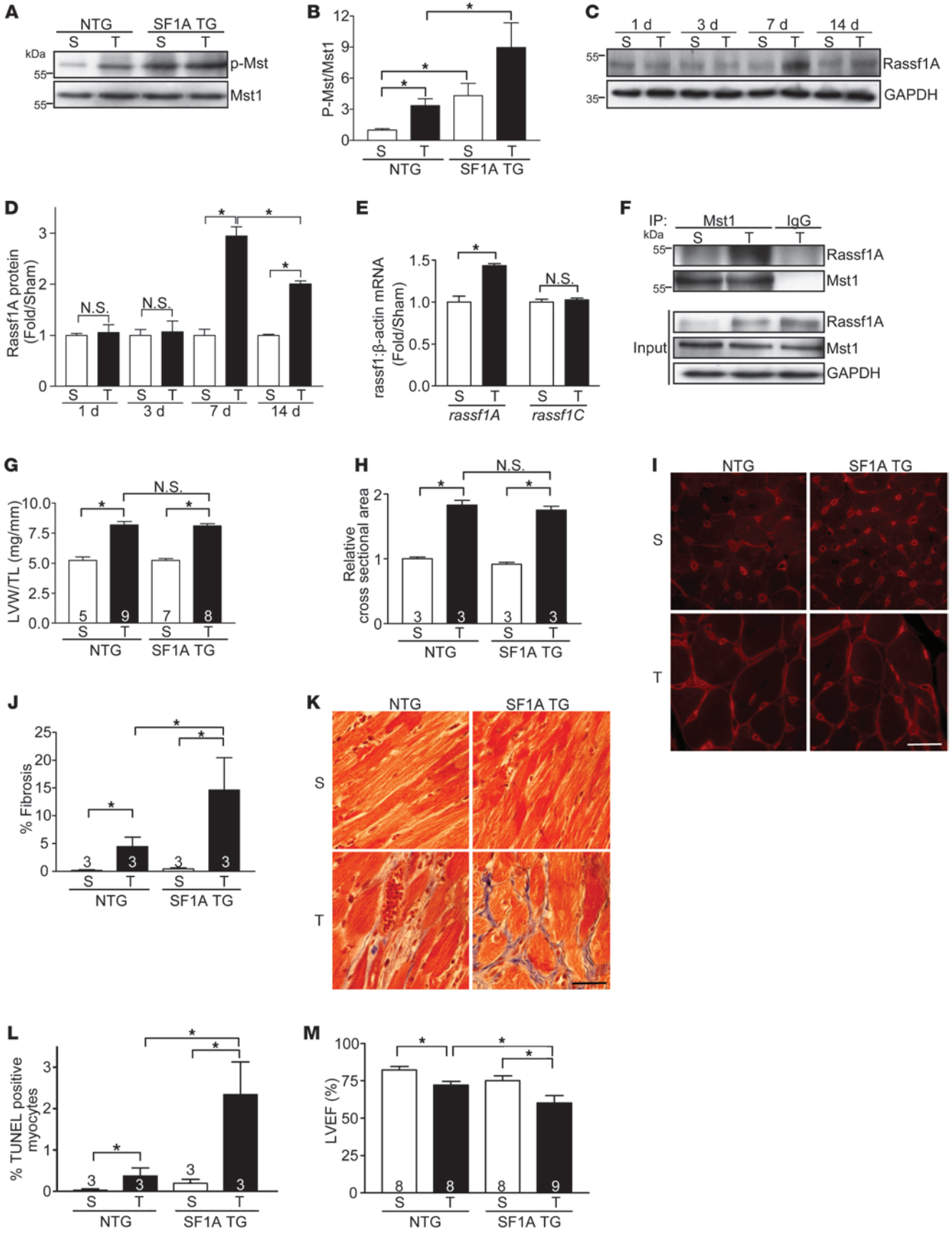
A
NTG
SF1A TG
S
T
S
T
kDa
55
p-Mst
55
Mst1
B
P-Mst/Mst1
12
9
6
3
0
*
*
*
S
T
S
T
NTG
SF1A TG
C
1 d
3 d
7 d
14 d
S
T
S
T
S
T
S
T
55
Rassf1A
35
GAPDH
D
Rassf1A protein (Fold/Sham)
3
2
1
0
N.S.
N.S.
*
*
*
S
T
S
T
S
T
S
T
1 d
3 d
7 d
14 d
E
rassf1:β-actin mRNA (Fold/Sham)
1.5
1.0
0.5
0.0
*
N.S.
S
T
S
T
rassf1A
rassf1C
F
IP:
Mst1
IgG
kDa
S
T
T
55
Rassf1A
55
Mst1
Input
Rassf1A
Mst1
GAPDH
G
LVW/TL (mg/mm)
10.0
7.5
5.0
2.5
0.0
*
N.S.
*
5
9
7
8
S
T
S
T
NTG
SF1A TG
H
Relative cross sectional area
2
1
0
*
N.S.
*
3
3
3
3
S
T
S
T
NTG
SF1A TG
I
NTG
SF1A TG
S
T
J
% Fibrosis
25
20
15
10
5
0
*
*
*
3
3
3
3
S
T
S
T
NTG
SF1A TG
K
NTG
SF1A TG
S
T
L
% TUNEL positive myocytes
3
2
1
0
*
*
*
3
3
3
3
S
T
S
T
NTG
SF1A TG
M
LVEF (%)
100
75
50
25
0
*
*
*
8
8
8
9
S
T
S
T
NTG
SF1A TG

Figure 1
Rassf1A exacerbates pressure overload–induced cardiac dysfunction. TAC was performed to generate pressure overload for 4 weeks (**A**, **B**, and **G**–**M**), 1 week (**E** and **F**), or as indicated (**C** and **D**). (**A**) Representative immunoblot demonstrating increased Mst1 phosphorylation in Rassf1A TG (SF1A TG) versus NTG hearts. S, sham; T, TAC. (**B**) Quantification of immunoblot results ($n = 3$). Values are relative to sham-operated NTG. (**C**) Representative immunoblot of Rassf1A protein expression in adult mouse heart after 1, 3, 7, and 14 day TAC versus sham operation. (**D**) Quantification of immunoblot results ($n = 3$). (**E**) Quantitative PCR results from cardiac tissue demonstrated upregulation of *rassf1A*, but not *rassf1C*, mRNA after 1 week TAC. (**F**) Representative immunoprecipitation of Mst1 from cardiac tissue showed interaction between endogenous Rassf1A and Mst1 in response to pressure overload. (**G**) LVW/TL showed no significant difference between NTG and TG groups. (**H**) Cardiomyocyte cross-sectional area; values are relative to sham-operated NTG. (**I**) Wheat germ agglutinin–stained representative images showed no difference in area between NTG and TG groups. (**J**) Fibrosis was assessed by Masson trichrome staining and fibrotic area determined. (**K**) Representative images show a marked increase in fibrosis in TG versus NTG hearts after pressure overload. (**L**) Increased cardiomyocyte apoptosis in TG versus NTG hearts after pressure overload, as determined by TUNEL staining. (**M**) Echocardiographic analysis of hearts. Data are mean ± SEM; numbers within bars denote *n*. $^*P < 0.05$. Scale bars: 100 μm.

of Rassf1A/Mst1 in fibroblasts was detrimental because it stimulated secretion of TNF-α, which in turn enhanced cardiac hypertrophy through a paracrine mechanism. Our results suggest that the functional significance of the Rassf1A/Mst1 pathway, one of the most prominent signaling mechanisms controlling apoptosis and cell growth in the heart, is quite opposite between cardiomyocytes and fibroblasts; we believe this represents a novel example of cardiac injury exacerbation via inhibition of cardiac fibroblast apoptosis.

Results

Rassf1A is upregulated by cardiac stress. Earlier studies from our lab established that insults such as I/R injury (3) and MI (2) activate Mst1 in the heart. Here, we found that Mst1 activation — as assessed by kinase autophosphorylation — increased in response to pressure overload induced by transverse aortic constriction (TAC; Figure 1, A and B). Accordingly, we sought to determine whether pressure overload alters expression of Rassf1A. Recent work demonstrated decreased Rassf1A protein in mouse heart following long-term TAC (12 weeks) and in samples from human heart failure patients (23). To implicate a more causative role for Rassf1A in the progression to heart failure, we measured Rassf1A expression levels following 1, 3, 7, and 14 days of pressure overload. We found significant upregulation of Rassf1A protein (Figure 1, C and D) and *rassf1A* mRNA (Figure 1E) after 7 days of TAC, whereas expression of the *rassf1C* splice variant was unchanged (Figure 1E).

Rassf1A interacts with Mst1 in the heart. Lacking catalytic activity, Rassf1A is thought to exert its cellular effects by acting as a scaffold to mediate protein interactions, and localization of Rassf1A is likely to influence its action in the cell. Rassf proteins have been demonstrated previously to associate with Mst1/2 in transformed cell lines (17). Therefore, we sought to determine whether an interaction occurs in the heart. To test this, we subjected WT mice to sham operation or TAC for 1 week, and Mst1 was immunoprecipitated from cardiac tissue. Subsequent probing for Rassf1A revealed an interaction between these proteins following pressure overload (Figure 1F), demonstrating endogenous association in the heart.

To further confirm an interaction between Rassf1A and Mst1 in cardiomyocytes, we performed immunocytochemistry to detect Rassf1A and found cytosolic localization (Supplemental Figure 1A; supplemental material available online with this article; doi:10.1172/JCI43569DS1). Detection of Mst1 showed a similar distribution in the cell, and colocalization was observed (Supplemental Figure 1A). Using an adenoviral system, we expressed Rassf1A or (L308P)Rassf1A, which harbors a point mutation in its conserved SARAH domain, in combination with Mst1 and performed coimmunoprecipitations. Our findings demonstrated that Rassf1A, but not (L308P)Rassf1A, existed in a complex with Mst1 in primary cardiomyocytes (Supplemental Figure 1B).

Rassf1A activates Mst1 in cardiomyocytes. Importantly, the ability of Rassf1A to interact with Mst1 may be critical to induction of Mst1 activation. We found that expression of Rassf1A significantly increased autophosphorylation of Mst1, a response that was inhibited by coexpression of kinase-inactive (K59R) dominant-negative Mst1 (dnMST1), whereas expression of (L308P)Rassf1A did not (Supplemental Figure 1, C and D). Further, Rassf1A caused a significant decrease in cell surface area, decreased expression of the hypertrophic marker atrial natriuretic factor (ANF), and increased cardiomyocyte apoptosis (Supplemental Figure 1, E–G). These cellular responses were all prevented by dnMst1 coexpression, providing strong evidence of Mst1 involvement, and were consistent with previous reports in other cell types (20, 21). We also failed to observe an additive effect of Rassf1A and Mst1 coexpression, further supporting our hypothesis that Rassf1A and Mst1 signal in series.

Rassf1A exacerbates cardiac dysfunction in response to stress. To determine the effect of increased Rassf1A expression in vivo, transgenic (TG) mice were generated to express either Rassf1A or (L308P)Rassf1A driven by the α–myosin heavy chain (α-MHC) promoter, which elicits cardiomyocyte-specific gene expression. The lines examined had comparable levels of Rassf1A transgene expression (Supplemental Figure 2A and Supplemental Figure 3A). At 10 weeks of age, neither TG line had significant differences in gross cardiac morphology (data not shown), heart size, fibrosis, or function (as determined by LV ejection fraction [LVEF]; Supplemental Figure 2, B–D and F, and Supplemental Figure 3, B–D and F). Notably, baseline Mst1 phosphorylation in cardiac tissue of Rassf1A TG mice was elevated and corresponded with increased TUNEL-positive myocytes (Supplemental Figure 2, A and E). In contrast, (L308P)Rassf1A TG hearts showed no difference in baseline Mst1 phosphorylation or TUNEL-positive myocytes versus nontransgenic (NTG) controls (Supplemental Figure 3, A and E).

The TG mice were then subjected to pressure overload to determine the effect of increased Rassf1A expression in the context of cardiac stress. After 4 weeks of pressure overload, the cardiac phenotype of both Rassf1A TG and (L308P)Rassf1A TG mice was assessed. Neither line showed a significant difference in LV weight/tibia length ratio (LVW/TL) or cardiomyocyte cross-sectional area compared with NTG control mice, indicating an unaltered hypertrophic response at the time point examined (Figure 1, G–I, and Figure 2, C–E). There was, however, a striking increase in Mst1 phosphorylation, as well as cardiac fibrosis and cardiomyocyte apoptosis, following pressure overload in the Rassf1A TG mice versus NTG littermates (Figure 1, A, B, and J–L). Additionally, Rassf1A TG mice had significantly impaired cardiac function after pressure overload compared with controls (Figure 1M). These data demonstrated that increased Rassf1A expression in cardiomyocytes increases Mst1 activation and promotes cardiomyocyte apoptosis in vivo, leading to worsened cardiac performance.

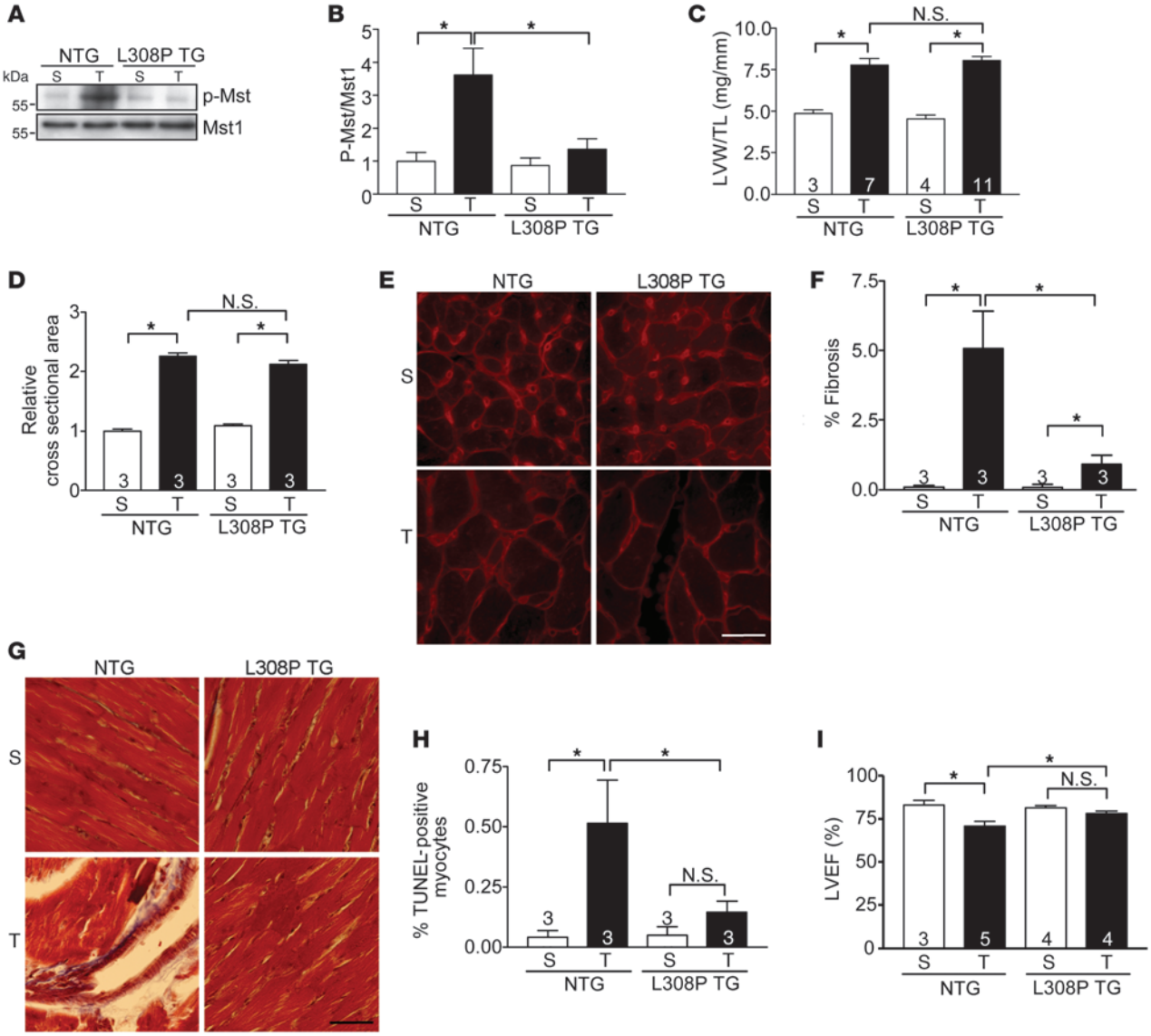

Figure 2

Mutant (L308P)Rassf1A protects against pressure overload–induced cardiac dysfunction. TAC was performed to generate pressure overload in vivo for 4 weeks. (**A**) Representative immunoblot demonstrating inhibition of Mst1 phosphorylation in (L308P)Rassf1A TG (L308P TG) versus NTG hearts. (**B**) Quantification of immunoblot results ($n = 3$). Values are relative to sham-operated NTG. (**C**) LVW/TL showed no difference between NTG and TG groups. (**D**) Cardiomyocyte cross-sectional area; values are relative to sham-operated NTG. (**E**) Wheat germ agglutinin–stained representative images showed no difference between NTG and TG hearts. (**F**) Fibrosis was assessed by Masson trichrome staining and fibrotic area determined. (**G**) Representative images show decreased fibrosis in TG versus NTG hearts after pressure overload. (**H**) Decreased cardiomyocyte apoptosis in TG versus NTG hearts after TAC, as assessed by TUNEL staining. (**I**) Echocardiographic analysis determined that LVEF was maintained in TG animals compared with NTG controls. Data are mean ± SEM; numbers within bars denote n. *$P < 0.05$. Scale bars: 100 μm.

The (L308P)Rassf1A mutant abolishes Mst1 activation and improves cardiac function. Interestingly, we observed a contrasting phenotype in (L308P)Rassf1A TG mice: after pressure overload, the level of phosphorylated Mst1 in (L308P)Rassf1A TG hearts was comparable to levels in sham-operated animals, indicative of near-complete abrogation of TAC-induced Mst1 activation (Figure 2, A and B). This result suggests that in addition to failing to activate Mst1 when expressed in the heart, (L308P)Rassf1A acts as a dominant-negative mutant, causing inhibition of endogenous Mst1 activation, after pressure overload. Additionally, the (L308P)Rassf1A TG mice showed significantly reduced fibrosis and cardiomyocyte apoptosis following pressure overload versus NTG controls (Figure 2, F–H). Importantly, LVEF was maintained in (L308P)Rassf1A TG mice compared with sham-operated animals and was significantly greater than that in TAC-operated NTG controls (Figure 2I). Thus, although increased cardiomyocyte expression of Rassf1A exacerbated cardiac dysfunction caused by pressure overload, expression of (L308P)Rassf1A prevented endogenous Mst1 activation, preserved function, and protected the heart. Taken together, these data implicate Mst1 as a critical effector of Rassf1A in vivo.

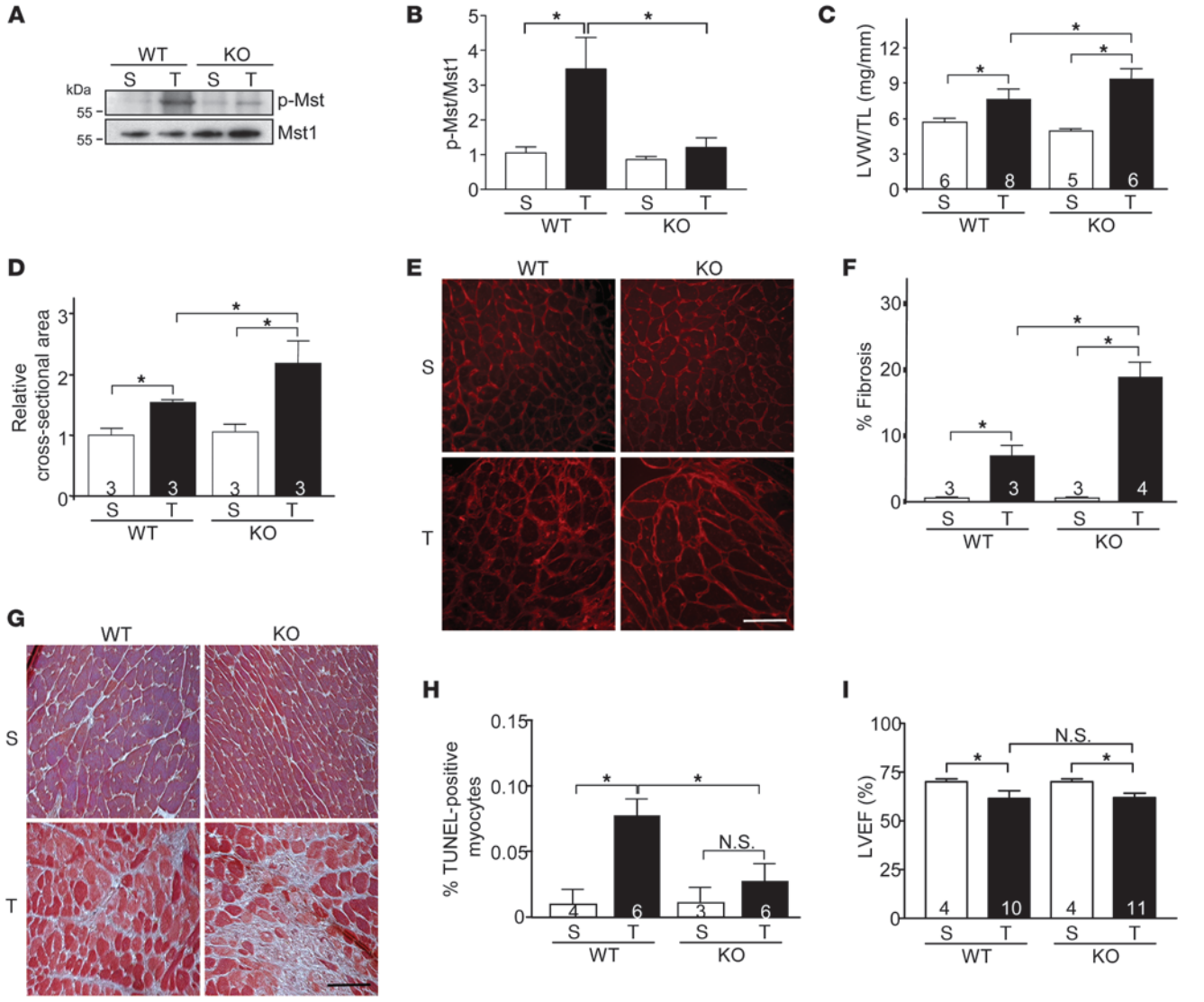

Figure 3

Systemic ablation of *rassf1A* causes exaggerated stress-induced hypertrophy and fibrosis in the heart. TAC was performed to generate pressure overload in vivo for 1 week. (**A**) Representative immunoblot demonstrated abolished Mst1 phosphorylation in *rassf1A* systemic KO versus WT hearts. (**B**) Quantification of immunoblot results ($n = 3$). Values are relative to sham-operated WT. (**C**) LVW/TL demonstrated increased cardiac hypertrophy in KO mice after TAC. (**D**) Cardiomyocyte cross-sectional area (shown relative to sham-operated WT) showed increased myocyte area in KO hearts after TAC. (**E**) Wheat germ agglutinin–stained representative images. (**F**) Fibrosis was assessed by Masson trichrome staining and fibrotic area determined. (**G**) Representative images showing exaggerated fibrosis in KO versus WT hearts. (**H**) Decreased cardiomyocyte apoptosis in KO versus WT hearts, as assessed by TUNEL staining. (**I**) Echocardiographic analysis. Data are mean ± SEM; numbers within bars denote *n*. $^*P < 0.05$. Scale bars: 100 μm.

Systemic ablation of rassf1A exaggerates the fibrotic response in the heart. To investigate the function of endogenous Rassf1A in the heart, systemic disruption of the *rassf1A* gene was achieved as described previously (12). Immunoblot analysis confirmed the complete absence of Rassf1A protein in the adult mouse heart (Supplemental Figure 4A). Baseline analysis revealed no significant difference in cardiac postmortem measurements of adult *rassf1A* KO mice versus WT littermates (Supplemental Figure 4, B–F). Function of adult *rassf1A* KO hearts was also assessed by hemodynamic analysis and was comparable to WT control mice at baseline (Supplemental Table 1).

As described above, our findings demonstrated upregulation of endogenous Rassf1A in response to pressure overload. We therefore subjected *rassf1A* KO mice to pressure overload to determine its role in pressure overload–induced cardiomyopathy. The increase in Mst1 phosphorylation observed in WT mouse hearts following TAC was nearly abolished in KO mice (Figure 3, A and B). This correlated with a significant increase in LVW/TL and myocyte cross-sectional area in KO versus WT mice (Figure 3, C–E), implicating Rassf1A as an endogenous inhibitor of the hypertrophic response to increased cardiac stress. A significant reduction in TUNEL-positive cardiomyocytes was observed in KO compared

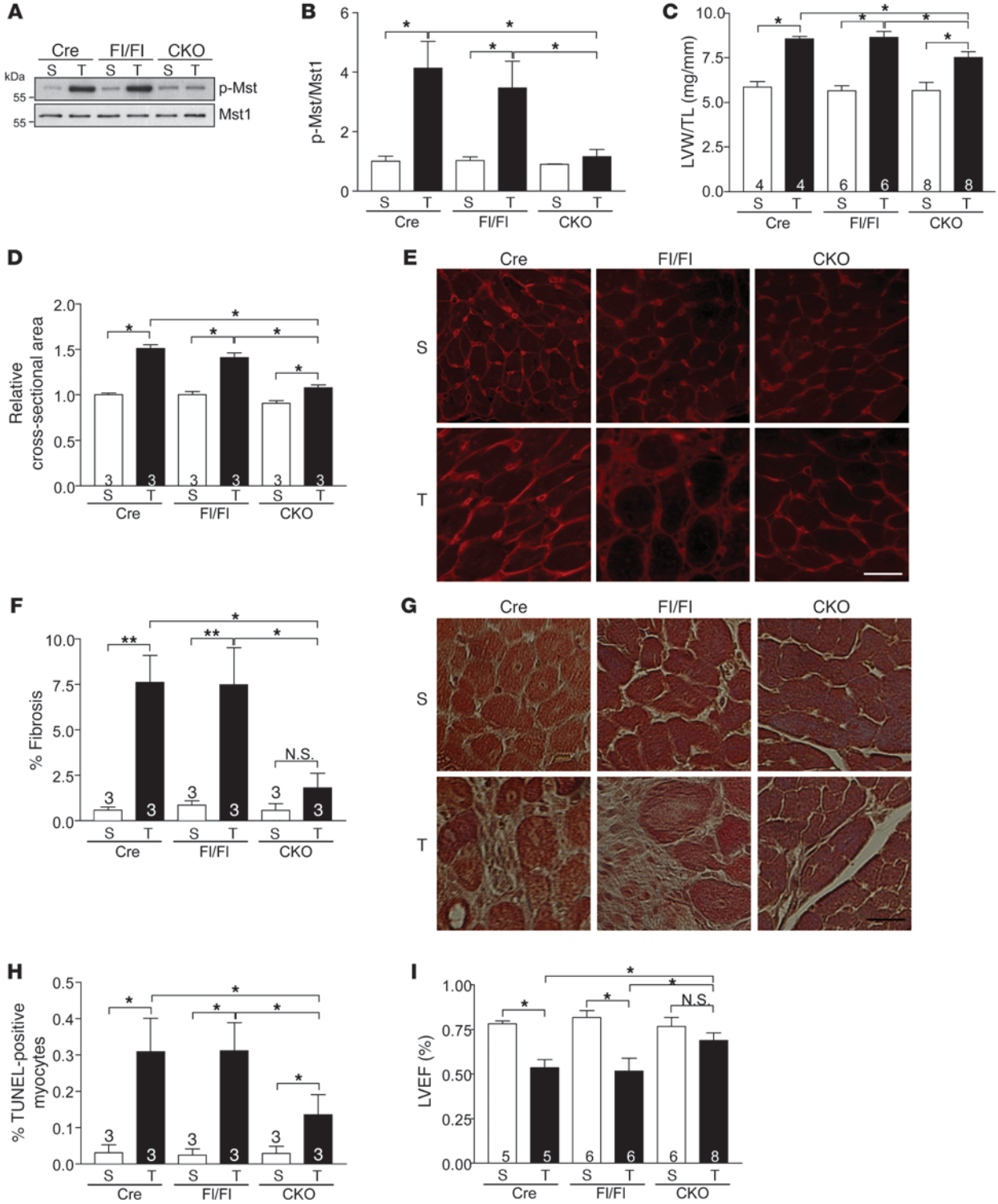

Figure 4

Cardiomyocyte-specific deletion of *rassf1A* attenuates hypertrophy and fibrosis caused by pressure overload. TAC was performed to generate pressure overload in vivo for 1 week. (**A**) Representative immunoblot demonstrating decreased Mst1 phosphorylation in *rassf1A* CKO versus α-MHC-Cre TG (Cre) and *rassf1A*$^{fl/fl}$ (Fl/Fl) hearts. (**B**) Quantification of immunoblot results ($n = 3$). Values are relative to sham-operated α-MHC-Cre TG. (**C**) Decreased hypertrophic response in CKO hearts after pressure overload. (**D**) Cardiomyocyte cross-sectional area. (**E**) Wheat germ agglutinin–stained representative images demonstrated attenuated myocyte growth in CKO hearts after TAC. (**F**) Fibrosis was assessed by Masson trichrome staining and fibrotic area determined. *rassf1A* CKO hearts had less fibrosis after pressure overload than did controls. (**G**) Representative images. (**H**) Decreased cardiomyocyte apoptosis in CKO versus control hearts after TAC, as assessed by TUNEL staining. (**I**) Echocardiographic analysis demonstrated preserved LVEF in CKO hearts after pressure overload. Data are mean ± SEM; numbers within bars denote *n*. $^*P < 0.05$; $^{**}P < 0.01$. Scale bars: 100 μm.

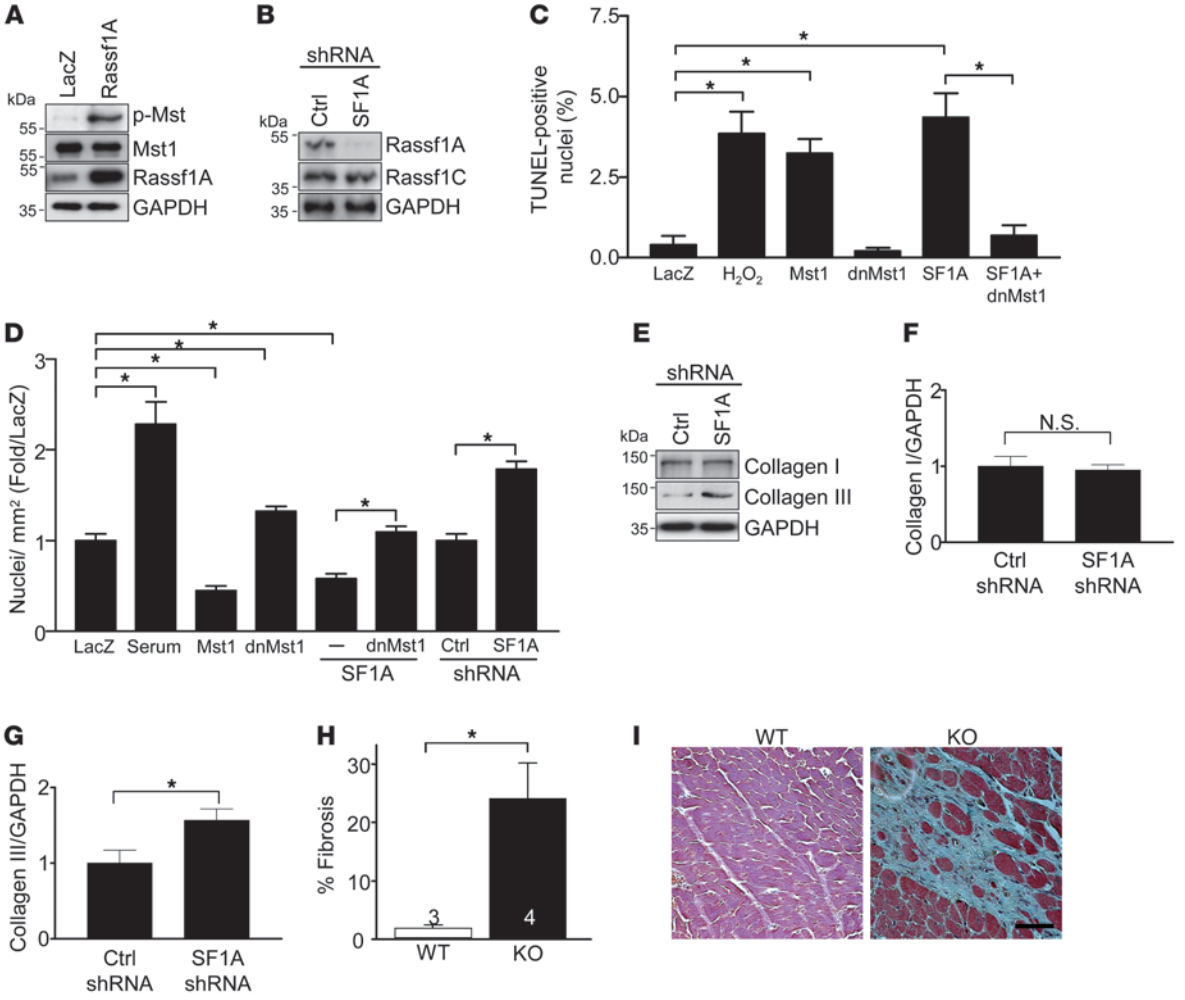

Figure 5

Endogenous Rassf1A represses cardiac fibroblast proliferation. (**A**–**G**) Fibroblasts were isolated from neonatal rat hearts and passaged a minimum of 3 times prior to experimentation. (**A**) Representative immunoblot demonstrating that Rassf1A overexpression increased Mst1 phosphorylation in cardiac fibroblasts. (**B**) Representative immunoblot demonstrating effectiveness and specificity of shRNA targeted to Rassf1A. (**C**) Fibroblasts were treated with H_2O_2 (100 μM) for 8 hours or adenovirus for 48 hours. TUNEL staining was performed to quantify apoptosis ($n = 3$). (**D**) Fibroblasts were treated with 10% FBS or adenovirus for 48 hours and then costained with anti-tubulin Ab and DAPI. Nuclei per ×10 visual field were counted, and the number per square millimeter was represented as fold of LacZ control ($n = 3$). (**E**) Representative immunoblot demonstrating increased collagen type III expression in response to Rassf1A depletion. (**F** and **G**) Quantitation of collagen type I and III expression ($n = 3$). Values are relative to control shRNA. (**H** and **I**) *rassf1A* KO mice were sacrificed at 10 months of age. (**H**) Significantly increased fibrotic area in KO versus WT hearts. Numbers within bars denote *n*. (**I**) Representative images. Data are mean ± SEM. *$P < 0.05$. Scale bar: 100 μm.

with WT mice after TAC, further evidence of the proapoptotic function of Rassf1A (Figure 3H). Unexpectedly, however, a striking increase in TAC-induced fibrosis was observed in KO versus WT hearts (Figure 3, F and G). Subsequently, we observed diminished LVEF in KO mice following pressure overload that was comparable to that of WT controls (Figure 3I). Intrigued by the exaggerated fibrosis observed in the KO mice, which was diametrically opposite to the decreased fibrosis found in the mutant (L308P)Rassf1A TG mice, we generated an alternate model to investigate the possible contribution of Rassf1A signaling in nonmyocytes.

Cardiomyocyte-specific deletion of rassf1A inhibits fibrosis and improves function. Given the lack of tissue specificity of the systemic KO model, we created a conditional deletion mutant using the Cre-lox system to achieve cardiomyocyte-specific (α-MHC-Cre) gene ablation (12). Adult *rassf1A* cardiomyocyte-specific KO (CKO) mice showed no obvious cardiac phenotype or functional abnormalities at baseline (Supplemental Figure 5 and Supplemental Table 2). We then subjected the CKO mice to pressure overload. Interestingly, although the increase in Mst1 phosphorylation observed in control hearts (α-MHC-Cre TG and *rassf1A*$^{fl/fl}$) following TAC was prevented to a similar extent in CKO and KO hearts (compare Figure 4, A and B, with Figure 3, A and B), the hypertrophic response to TAC was significantly attenuated in CKO mice versus controls (Figure 4, C–E). Furthermore, we observed a significant reduction in cardiac fibrosis in CKO hearts following TAC compared with control hearts (Figure 4, F and G). Inhibition of cardiomyocyte apoptosis following pressure overload was comparable between CKO and KO mice (compare Figure 4H with Figure 3H), but cor-

related with improved LVEF only in CKO mice (compare Figure 4I with Figure 3I). These hypertrophy, fibrosis, and functional data were in sharp contrast with our findings in *rassf1A* KO mice, demonstrating the critical importance of nonmyocytes in mediating these stress-induced responses.

Mst1 mediates inhibition of NF-κB in cardiac fibroblasts. The opposing hypertrophic and fibrotic phenotypes observed in *rassf1A* KO versus CKO mice led us to examine the function of Rassf1A signaling in cardiac fibroblasts. Closer examination of activated Mst1 protein using immunohistochemistry revealed TAC-induced Mst1 phosphorylation in nonmyocytes in CKO hearts; however, phosphorylated Mst1 was not observed in KO hearts (Supplemental Figure 6), which suggests that endogenous Rassf1A in nonmyocytes of CKO hearts sustains Mst1 activation. Isolated primary rat cardiac fibroblasts were transduced to express either WT Rassf1A or Rassf1A-specific shRNA to deplete endogenous Rassf1A protein (Figure 5, A and B). Increased expression of Rassf1A caused increased Mst1 phosphorylation and promoted Mst1-mediated apoptosis, while significantly impairing the ability of fibroblasts to proliferate (Figure 5, A, C, and D). Conversely, knockdown of Rassf1A promoted fibroblast proliferation, suggestive of inhibited proliferation by endogenous Rassf1A (Figure 5D). We also observed modestly increased expression of collagen type III, but not type I, in response to Rassf1A depletion (Figure 5, E–G). This was further supported by our finding that aged *rassf1A* KO mice showed increased fibrosis under basal conditions (Figure 5, H and I) and correlated with worsened heart function compared with WT mice, whereas cardiac function of aged *rassf1A* CKO mice was normal (data not shown). The putative transcription factor NF-κB is an important mediator of cardiac hypertrophy and fibrosis following insult (24). To determine whether Rassf1A modulates NF-κB activation in fibroblasts, a luciferase reporter assay was performed. Although increased Rassf1A expression had no effect, knockdown of Rassf1A was sufficient to activate endogenous NF-κB, a response that was abolished by increased expression of Mst1 (Figure 6A). Furthermore, shRNA directed at Rassf1A caused an increase in phosphorylation of IKKα/β and Akt (Figure 6B), a known upstream activator of the IKK complex (25, 26), as well as the p65 subunit of NF-κB (Supplemental Figure 7A). Inhibition of Mst1 also activated NF-κB, mimicking the response seen during Rassf1A depletion (Supplemental Figure 7B). These data strongly indicate that Rassf1A promotes inhibition of NF-κB in cardiac fibroblasts and that this response is mediated by Mst1.

Rassf1A depletion upregulates TNF-α expression. We performed a quantitative cytokine PCR array to screen for changes in expression of 89 target genes using primary cardiac fibroblasts transduced with either scrambled control or Rassf1A-specific shRNA. The results indicated that TNF-α mRNA was upregulated nearly 40-fold in Rassf1A-depleted fibroblasts compared with control cells (data not shown). This increase in TNF-α mRNA expression was subsequently confirmed by RT-PCR (Figure 6C). Importantly, we also confirmed no changes in mRNA expression of IL-6 or IL-1β, 2 NF-κB responsive genes, nor did we observe any change in TGF-β1 transcript, a known profibrotic mediator, further evidence that Rassf1A depletion in fibroblasts leads to selective upregulation of TNF-α (Figure 6C).

TNF-α mediates autocrine/paracrine effects of Rassf1A knockdown. We hypothesized that cardiac fibroblasts lacking Rassf1A express and secrete TNF-α, thereby stimulating cardiomyocyte growth in a paracrine manner. To test this, ELISA was performed to detect TNF-α protein in conditioned media from control and Rassf1A shRNA–treated fibroblasts. Our results demonstrated a significant increase in TNF-α protein secretion following Rassf1A depletion or Mst1 inhibition (Figure 6D). Media was collected from cells treated with control or Rassf1A shRNA and incubated with vehicle, IgG control, or TNF-α neutralizing Ab (TAb) before transfer to cardiomyocytes. We found that conditioned media recovered from fibroblasts treated with Rassf1A shRNA stimulated increased cardiomyocyte cell surface area, protein content, and ANF expression compared with media from fibroblasts treated with control shRNA (Figure 6, E–G). Treatment of conditioned media with IgG Ab had no effect; however, TAb significantly attenuated cardiomyocyte growth elicited by conditioned media from Rassf1A shRNA–treated fibroblasts (Figure 6, E–G). We also used adenoviral expression of a nonphosphorylatable IκBαSA mutant (27) to selectively inhibit NF-κB activation (Supplemental Figure 7A). Similarly, medium collected from fibroblasts cotransduced with Rassf1A shRNA and IκBαSA was unable to stimulate cardiomyocyte growth, as measured by cell area, protein content, and ANF expression (Figure 6, E–G), implicating NF-κB activity as necessary for this paracrine response. Importantly, we also sought to determine whether secreted TNF-α stimulates autocrine-mediated fibroblast proliferation. Application of conditioned media to fibroblasts promoted NF-κB/TNF-α–dependent proliferation (Figure 6H), confirming a positive feedback mechanism regulated by Rassf1A.

Neutralizing TNF-α in vivo rescues rassf1A KO hearts. Having established the importance of Rassf1A signaling in fibroblast survival, proliferation, and TNF-α production, we sought to determine whether the same mechanism functions in vivo. TNF-α expression increased in hearts from KO mice after pressure overload compared with WT hearts, whereas CKO hearts produced less TNF-α than did littermate controls (Figure 7, A and C). Analysis of sections from these hearts revealed an increase in the presence of nonmyocytes staining positive for TNF-α in KO versus WT mice after TAC (Figure 7B). Interestingly, a decrease in TNF-α–positive nonmyocytes was observed in *rassf1A* CKO hearts after TAC compared with control hearts (Figure 7D). To further establish the role of fibroblasts in mediating increased TNF-α expression in *rassf1A* KO hearts, sections from KO and WT hearts were costained with the fibroblast marker anti-Hsp47 and with anti–TNF-α. Importantly, we observed more Hsp47 and TNF-α double-positive cells in KO versus WT hearts following pressure overload, which suggests that the critical cell type is in fact the fibroblast (Supplemental Figure 8).

To test the importance of fibroblast-secreted TNF-α in the exaggerated growth and fibrotic responses in KO mice following pressure overload, TAb or IgG control was administered to WT and KO mice immediately following TAC and again 48 hours after surgery. Subsequently, LVW/TL and myocyte cross-sectional area were compared between all groups. Postmortem measurements indicated that treatment with TAb significantly attenuated the exaggerated hypertrophic response observed in *rassf1A* KO hearts following pressure overload compared with IgG control administration (Figure 7, E–G). Importantly, TAb normalized the extent of fibrosis observed in KO hearts to control levels (Figure 7, H and I). In addition, the cardiac function determinants lung weight/tibia length ratio and LVEF were both improved in TAb-treated animals following pressure overload (Figure 7, J and K). Taken together, these data strongly implicate TNF-α as a key molecule in mediating increased cardiomyocyte growth and increased cardiac fibrosis following pressure overload in mice lacking *rassf1A*.

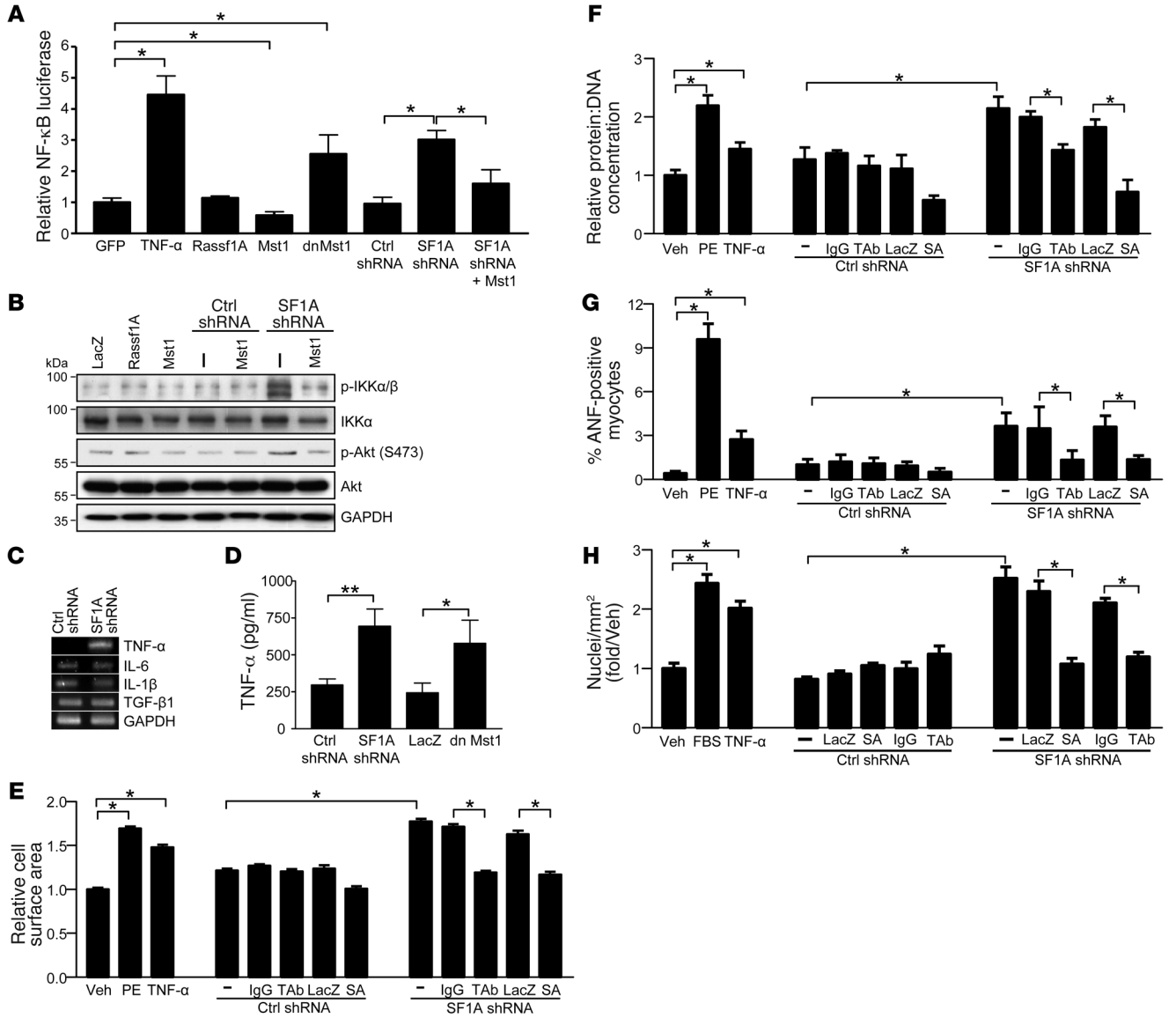

Figure 6

rassf1A silencing stimulates TNF-α to promote autocrine-mediated fibroblast proliferation and paracrine-mediated cardiomyocyte hypertrophy. (**A**) Luciferase reporter assay demonstrated the ability of endogenous Rassf1A to inhibit *nf-κb* promoter activation. Values are relative to GFP. (**B**) Representative immunoblot demonstrating activation of Akt and IKK complex in response to Rassf1A depletion. (**C**) RT-PCR performed with fibroblast mRNA demonstrated selective upregulation of TNF-α mRNA. (**D**) TNF-α was detected in medium of fibroblasts by ELISA 48 hours after Rassf1A depletion or dnMst1 expression. (**E**–**G**) Cardiac fibroblasts were treated with adenovirus expressing scrambled control or Rassf1A shRNA, alone or in combination with LacZ or IκBαSA (SA) mutant, and the resulting conditioned medium was transferred to serum-starved cardiomyocytes. Conditioned medium from control and Rassf1A shRNA–treated cells was also incubated with mouse IgG or TAb (100 ng/ml) for 30 minutes prior to transfer. Values are shown relative to vehicle control. (**E**) Cells were stained with α-actinin Ab and surface area determined. (**F**) Total protein content was normalized to DNA content. (**G**) Cardiomyocytes were stained with ANF Ab and positive cells counted. (**H**) Cardiac fibroblasts and conditioned media were treated as described above, and the resulting conditioned media were transferred to separate serum-starved fibroblasts. Cells were costained with anti-tubulin Ab and DAPI. Nuclei per ×10 visual field were counted, and the number per square millimeter was expressed as fold of vehicle control. Treatment with TNF-α (10 U/ml), PE (100 μm), and serum (10% FBS) served as controls. Data are mean ± SEM ($n = 3$). $^*P < 0.05$; $^{**}P < 0.01$.

Discussion

Mst1 is an important regulator of mammalian cell growth and survival (28). Mst kinases are able to promote cell cycle arrest and apoptosis through phosphorylation of several known substrates, including histone H2B (29), FOXO3 (30), Lats1/2 (31), JNK, and p38 (32). Stimuli that induce apoptosis, such as UV radiation, reactive oxygen species, and serum starvation, cause autophosphorylation and activation of Mst1 through mechanisms still largely unknown (9). The tumor suppressor Rassf1A has been implicated in Mst1 regulation, although its role has yet to be clearly defined, and previous studies are conflicting (19–22). Still other work suggests that the Rassf family member NORE1 is important in regulating Mst1 activity (17, 33).

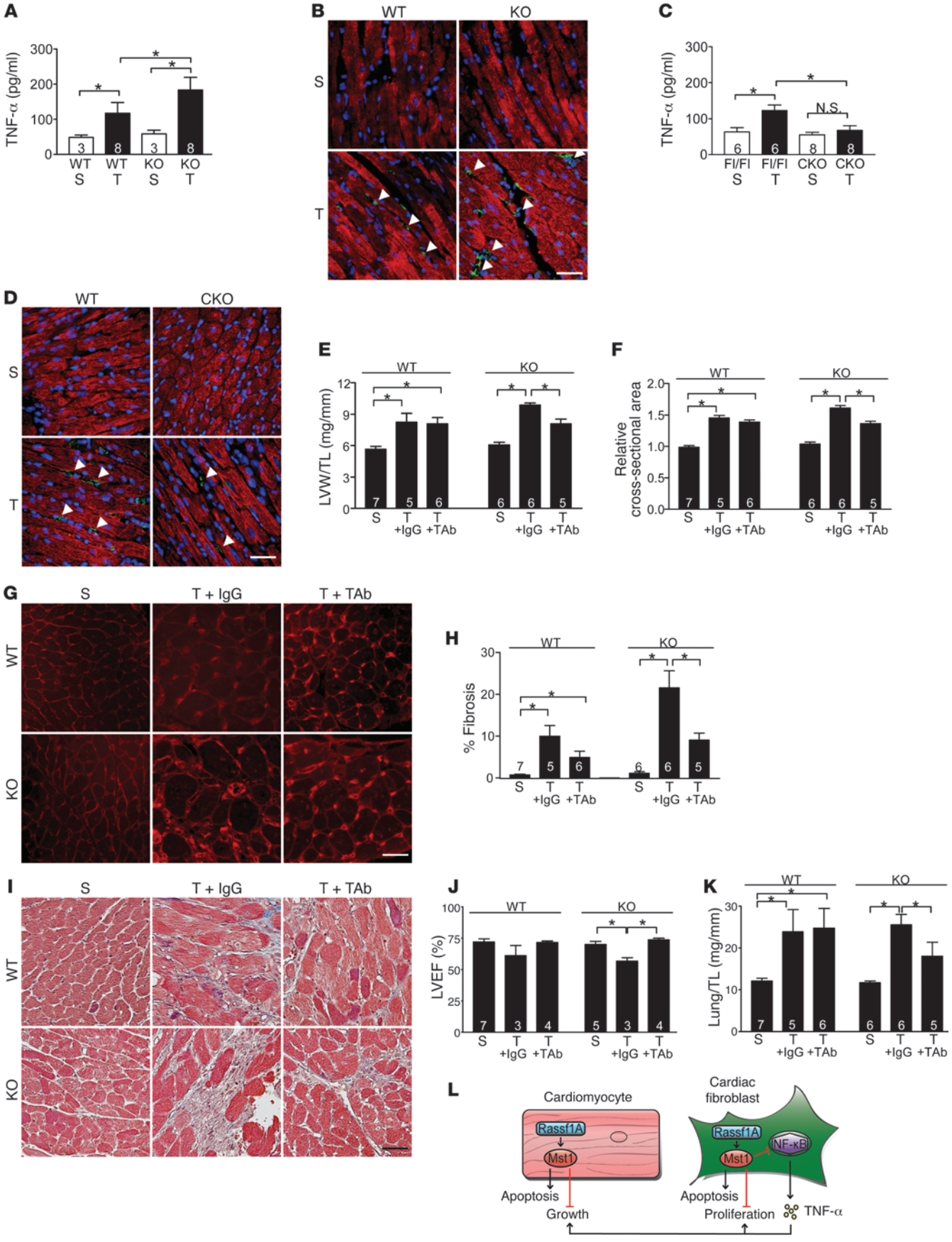
A
TNF-α (pg/ml)
300
200
100
0
WT S
WT T
KO S
KO T
B
WT
KO
S
T
C
TNF-α (pg/ml)
N.S.
Fl/Fl S
Fl/Fl T
CKO S
CKO T
D
WT
CKO
S
T
E
LVW/TL (mg/mm)
WT
KO
S
T +IgG
T +TAb
F
Relative cross-sectional area
G
S
T + IgG
T + TAb
WT
KO
H
% Fibrosis
I
J
LVEF (%)
K
Lung/TL (mg/mm)
L
Cardiomyocyte
Rassf1A
Mst1
Apoptosis
Growth
Cardiac fibroblast
NF-κB
Proliferation
TNF-α

Figure 7
TNF-α mediates the effects of Rassf1A in vivo. (**A**–**K**) TAC was performed to generate pressure overload in vivo for 1 week. (**A** and **C**) Whole hearts were removed and homogenized, and TNF-α concentration was determined by ELISA. (**B** and **D**) Representative images detecting troponin T (cardiomyocytes, red) and TNF-α (green). Increased TNF-α was detected in *rassf1A* KO versus WT hearts, whereas less TNF-α was observed in *rassf1A* CKO versus *rassf1A*$^{fl/fl}$ hearts (arrowheads). (**E**–**K**) WT and KO mice were subjected to sham operation or to TAC in combination with either control IgG or TAb (3 mg/kg) treatment. (**E**) Postmortem analysis showed LVW/TL normalization in KO mice treated with TAb. (**F**) Cardiomyocyte cross-sectional area (shown relative to sham operation) was determined using wheat germ agglutinin staining. TAb treatment normalized myocyte area in KO hearts after TAC. (**G**) Representative images. (**H**) Fibrosis was assessed by Masson trichrome staining, and fibrotic area showed reduced fibrosis in KO hearts with TAb administration. (**I**) Representative images. (**J**) Echocardiographic analysis demonstrated improved LVEF in KO mice given TAb but not IgG control. (**K**) Lung weight/tibia length ratio (Lung/TL) decreased in KO mice treated with TAb versus control IgG after pressure overload. Data are mean ± SEM; numbers within bars denote *n*. **P* < 0.05. Scale bars: 100 μm. (**L**) Proposed schema depicting Rassf1A/Mst1 signaling in cardiomyocytes and cardiac fibroblasts.

Our findings presented here demonstrate the ability of endogenous Rassf1A to mediate Mst1 activation in vivo. Importantly, we observed that cardiac stress caused increased association of endogenous Rassf1A and Mst1. We demonstrate that this association is critical to mediate activation of Mst1, as transgenic expression of Rassf1A induced activation of endogenous Mst1, whereas expression of (L308P)Rassf1A — which cannot bind Mst1 — did not activate this kinase. Using primary cell cultures, we demonstrated this observation held true in both cardiomyocytes and cardiac fibroblasts, providing strong evidence that Rassf1A functions as a promoter of Mst1 activation in the heart. Our findings, however, do not exclude the possibility that other Rassf family members may be involved in this signaling pathway in the heart or other cell types (14).

Whereas cardiomyocytes make up the bulk of cardiac mass, fibroblasts constitute the majority cell type in the adult heart and are critical to normal heart function (34, 35). Upon activation, fibroblasts proliferate, migrate, and secrete various factors, including TNF-α (36). Although persistent fibroblast activation is thought to facilitate scarring and fibrosis, ultimately leading to compromised cardiac function, the role of these cells in cardiac pathophysiology is still not fully understood. Here we identified Rassf1A as a critical regulator of fibrosis via activation of Mst1 and repression of NF-κB signaling, collagen expression, and fibroblast proliferation, evidence of Rassf1A/Mst1 involvement in this pathophysiological response.

Surprisingly, we found that heart size and fibrosis were dramatically increased in mice with systemic deletion of *rassf1A*, whereas hearts from mice with cardiomyocyte-restricted deletion of *rassf1A* were smaller and less fibrotic. This observation led us to investigate the cell type specificity of Rassf1A signaling in the heart. Interestingly, we found that Rassf1A in cardiomyocytes primarily induced apoptosis, but also inhibited hypertrophic cell growth, whereas in cardiac fibroblasts, it primarily suppressed cell proliferation while also promoting apoptosis. The low proliferative potential of differentiated cardiomyocytes may explain why Rassf1A primarily affects apoptosis and growth rather than proliferation in cardiomyocytes. The ability of the Mst1 homolog Hippo to inhibit cell proliferation and promote apoptosis, thereby limiting organ size, was first described in *Drosophila* (37, 38), and recent work has demonstrated a similar phenotype in mammals (39, 40). Our present work suggests that Rassf1A inhibits heart size not only through induction of cell death and inhibition of cell proliferation, but also by negatively regulating hypertrophic cell growth in individual cardiomyocytes, confirming our previous finding that Mst1/Lats2 inhibits cardiomyocyte size (4) and expanding the scope of growth inhibition by mammalian Hippo signaling.

Furthermore, we elucidated a mechanism involving both cell-autonomous and non–cell-autonomous effects to suppress cardiomyocyte growth and fibroblast proliferation. Silencing of *rassf1A* in isolated cardiomyocytes or in aged KO mice caused increased growth, which suggests that Rassf1A inhibits myocyte growth directly and indicates that disruption of *rassf1A* alone is sufficient to elicit this effect (data not shown). We also determined that cardiomyocyte growth was regulated in a paracrine manner through Rassf1A/Mst1-mediated inhibition of cardiac fibroblast TNF-α secretion — a factor shown previously to stimulate myocyte hypertrophy (41). In fact, we demonstrated that TNF-α protein levels were increased in *rassf1A* KO hearts and, importantly, that neutralization of TNF-α in vivo was sufficient to rescue the deleterious effects of systemic *rassf1A* ablation following cardiac stress. Regulation of organ size by non–cell-autonomous mechanisms has not been demonstrated in the *Drosophila* Hippo pathway, indicative of the complexity present in mammalian Mst1 signaling. Additionally, we showed that the subsequent upregulation of TNF-α in response to *rassf1A* deletion in fibroblasts also triggered autocrine-mediated proliferation, thereby promoting an active fibrotic process and deterioration of organ function.

We believe these findings facilitate both the increased fibrosis and exaggerated hypertrophic response observed in systemic *rassf1A* KO mouse hearts in response to pressure overload. Surprisingly, we found that cardiac hypertrophy was significantly reduced in CKO versus control mice following stress. We propose that the inhibition of fibrosis and maintained function observed in CKO hearts is sufficient to prevent stress-induced compensatory growth, resulting in attenuated cardiac hypertrophy. Furthermore, CKO hearts produced less TNF-α and exhibited reduced neutrophil recruitment compared with their control counterparts (data not shown), which suggests that hereto undefined stimulatory cross-talk from myocyte to fibroblast occurs and is diminished in the CKO heart.

Our findings establish that Rassf1A is an endogenous activator of Mst1, thus mediating cell type–specific effects that lead to distinct functional outcomes: in cardiomyocytes, increased Rassf1A expression activates Mst1 to inhibit cell growth and promote apoptosis; however, Rassf1A in cardiac fibroblasts prevents cell proliferation while inducing apoptosis via Mst1 (Figure 7L). We therefore propose that selective inhibition of Rassf1A/Mst1 signaling in cardiomyocytes may prove most beneficial as a therapeutic strategy. This would prevent cardiomyocyte apoptosis, while the maintained Rassf1A/Mst1 function in cardiac fibroblasts should serve to suppress fibrosis following stress and improve cardiac function. Addressing the issue of cell-specific signaling raises the intriguing possibility that apoptosis of certain cell types (e.g., fibroblasts) could prove beneficial following cardiac insult. Thus, cell-specific targeting remains critical, as the overall effect of Rassf1A may be determined by the balance between its proapoptotic function in myocytes and its antifibrotic effect. If our hypothesis is true, suppressing cardiomyocyte Rassf1A alone may prove superior to inhibiting ubiquitous Rassf1A function as a treatment for heart failure.

Methods

Animal models. Rassf1A TG and mutant (L308P)Rassf1A TG mice were generated (FVB/N background) using cDNA of human HA-Rassf1A and HA-Rassf1A (L308P) driven by the α-MHC promoter (provided by J. Robbins, University of Cincinnati, Cincinnati, Ohio, USA) to achieve cardiac-specific expression. Generation of *rassf1A* KO and *rassf1A* CKO (exon 1α) mice has been described previously (12). *rassf1A* CKO mice were bred with α-MHC-Cre transgenic mice (provided by M. Schneider, Imperial College, London, United Kingdom) to accomplish cardiomyocyte-specific disruption of the *rassf1A* gene. All protocols concerning the use of animals were approved by the Institutional Animal Care and Use Committee at the University of Medicine and Dentistry of New Jersey.

TAC. The method for imposing pressure overload in mice has been described previously (4). Briefly, mice were anesthetized with a mixture of ketamine, xylazine, and acepromazine and mechanically ventilated. The left chest was opened at the second intercostal space. Aortic constriction was performed by ligation of the transverse thoracic aorta with a 28-gauge needle using a 7-0 braided polyester suture. Sham operation was performed without constricting the aorta. For the TNF-α–neutralizing experiment, anti-mouse TAb (R&D Systems) or IgG control was administered (3 mg/kg) by i.p. injection immediately following TAC and 48 hours after operation.

Echocardiography. Mice were anesthetized using 12 μl/g body weight of 2.5% tribromoethanol (Avertin; Sigma-Aldrich), and echocardiography was performed as described previously (2) using a 13-MHz linear ultrasound transducer. 2-dimensional guided M-mode measurements of LV internal diameter were obtained from at least 3 beats and then averaged. LV end-diastolic dimension (LVEDD) was measured at the time of the apparent maximal LV diastolic dimension, and LV end-systolic dimension (LVESD) was measured at the time of the most anterior systolic excursion of the posterior wall. LVEF was calculated as $(LVEDD^3 - LVESD^3)/LVEDD^3$ and expressed as a percentage.

Histological analyses. Heart specimens were fixed with formalin, embedded in paraffin, and sectioned at 6-μm thickness. Interstitial fibrosis was evaluated by Masson trichrome staining as described previously (2). Myocyte cross-sectional area was measured from images captured from wheat germ agglutinin–stained sections as described previously (3).

Evaluation of apoptosis. DNA fragmentation was detected in situ and in cultured cells using TUNEL as described previously (2). Nuclear density was determined by counting DAPI-stained nuclei in 20 different fields for each sample.

Primary culture of neonatal rat cardiac myocytes and fibroblasts. Primary cultures of ventricular cardiomyocytes and cardiac fibroblasts were prepared from 1-day-old Crl: (WI) BR-Wistar rats (Harlan) as described previously (2, 42).

Construction of adenoviral vectors. We constructed recombinant adenovirus harboring WT HA-Rassf1A and mutant HA-Rassf1A (L308P) using an Adeno-X adenovirus construction kit (CLONTECH Laboratories Inc.). Adenovirus harboring β-galactosidase (LacZ) was used as a control. Generation of adenovirus harboring WT Mst1, dnMst1 (K59R), and dnIκBα (IκBαSA) have been described previously (2, 27). All adenoviruses were used at 10 MOI.

Construction of shRNA adenoviral expression vector. pSilencer 1.0-U6 expression vector was purchased from Ambion. The U6 RNA polymerase III promoter and the polylinker region were subcloned into the adenoviral shuttle vector pDC311 (Microbix). The hairpin-forming oligo, corresponding to bases 6–24 (5′-GGCGGAGCCAGAACTCATTTTCAAGAGAAATGAGTTCTGGCTCCGCCTTTTTA-3′; loop sequence underlined) of rat *rassf1A* cDNA, and its antisense with ApaI and Hind III overhangs were synthesized, annealed, and subcloned distal to the U6 promoter. Adenovirus harboring control shRNA has been described previously (4).

Immunoblot analysis. Cells were lysed in buffer containing 25 mmol/l NaCl, 25 mmol/l Tris (pH 7.4), 1 mmol/l Na_3VO_4, 10 mmol/l NaF, 10 mmol/l sodium pyrophosphate, 0.5 mmol/l EGTA, 0.5 mmol/l AEBSF, 0.5 μg/ml leupeptin, and 0.5 μg/ml aprotinin. For immunoblotting, antibodies against Mst1, phospho-Mst1/2 (T183/T180), Akt, phospho-Akt (S473), p65, phospho-p65 (S536), IKKα, phospho-IKKα/β (S180/S181), IκBα, and GAPDH were obtained from Cell Signaling Technology. Ab against Rassf1A was obtained from eBioscience. Rassf1C Ab was purchased from Abcam. Collagen type I Ab was purchased from Rockland. Collagen type III Ab was obtained from Chemicon. For immunoprecipitation experiments, immunocomplexes were precipitated using A/G sepharose (Santa Cruz). Densitometry was performed using AlphaEase FC software (Alpha Innotech).

ELISA. Medium from treated cells was collected, or ventricular tissue was homogenized, and TNF-α protein was measured according to the manufacturer's instructions (eBioscience). Recombinant TNF-α protein was purchased from Sigma-Aldrich.

Immunohistochemistry. Heart sections were stained with anti–TNF-α rabbit polyclonal Ab (Abcam), anti–troponin-T mouse mAb (Neomarkers), Alexa Fluor 488–conjugated goat anti-rabbit IgG (Invitrogen), Alexa Fluor 594–conjugated goat anti-mouse IgG (Invitrogen), and Vectashield mounting medium with DAPI (Vector Laboratories). Analyses were performed using fluorescence microscopy (Zeiss). See Supplemental Methods for details.

Quantitative real-time PCR. RNA was extracted from mouse ventricle (RNeasy Fibrous Tissue Mini Kit; Qiagen), and 2 μg total RNA was used to generate cDNA (M-MLV reverse transcriptase; Promega). Quantitative real-time PCR was performed using Maxima SYBR Green/ROX Master Mix (Fermentas) and the following primers: *rassf1A*, 5′-ATGTCGGCGGAGCCAGAACTCATTGAACTA-3′ and 5′-CACGTTCGTATCCCGCTCTAGTGCAGAGT-3′; *rassf1C*, 5′-ATGGGCGAGGCTGAAACACCTTCCTTCGAA-3′ and 5′-CAGGCTCATGAAGAGGTTGCTGTTGATCT-3′; β-*actin*, 5′-ACCAACTGGGACGATATGGAGAAGA-3′ and 5′-TACGACCAGAGGCATACAGGGACAA-3′. Melting curve analysis was performed to ensure purity of the PCR products, and relative quantitation was determined using the comparative C_T method.

Evaluation of cell surface area and total protein content. Cell surface area was measured using F-actin–stained cells and NIH Image software. F-actin was detected with TRITC-labeled phalloidin (Invitrogen). Total protein concentration per dish was determined as described previously (4).

Luciferase assay. The transcriptional activity of NF-κB was evaluated using a NF-κB–Luc reporter gene containing multiple NF-κB *cis* elements. Cells were transfected (Lipofectamine; Invitrogen), and luciferase activity was determined (Promega) as described previously (4). See Supplemental Methods for details.

RT-PCR. Total RNA was isolated from cardiac fibroblasts using TRIzol (Invitrogen), and RT-PCR was performed as described previously (43). The following primers were used: TNF-α forward, 5′-CCGGGTCTGGGAGTGTGAGT-3′; TNF-α reverse, 5′-CTCCTCCGCTTGGTGGTTTG-3′; IL-6 forward, 5′-TGAAGGTCGGTCAACGGAAGA-3′; IL-6 reverse, 5′-GTTATATCCAGTTTGGAAGCA-3′; IL-1β forward, 5′-CCTCTTACTGGACAAGAAACT-3′; IL-1β reverse, 5′-CTTCAAAGATGAAGGAAAAGA-3′; TGF-β1 forward, 5′-ATATCGTTGTTAAGGACCGCA-3′; TGF-β1 reverse, 5′-TGATTTCCACGTGGATTTGCT-3′; GAPDH forward, 5′-AGACAGCCGCATCTTCTTGT-3′; GAPDH reverse, 5′-CTTGCCGTGGGTAGAGTCAT-3′. In all cases, PCR of RNA samples was negative in the absence of RT (data not shown).

Immunocytochemistry, coimmunoprecipitation, and hemodynamic measurements. See Supplemental Methods.

Statistics. All data are reported as mean ± SEM. Statistical analyses between groups were done by 1-way ANOVA, and differences among group means were evaluated using Tukey's post-test. Student's *t* test (2-tailed) was used between data pairs. A *P* value less than 0.05 was considered significant.

Acknowledgments

The authors thank Daniela Zablocki for critical reading of the manuscript and Grace H. Lee for assistance in preparing the schema. This work was supported in part by U.S. Public Health

Service Grants HL099148, HL59139, HL67724, HL69020, HL91469, and AG27211. This work was also supported by Foundation Leducq Transatlantic Network of Excellence.

Received for publication May 2, 2010, and accepted in revised form August 9, 2010.

Address correspondence to: Junichi Sadoshima, Department of Cell Biology and Molecular Medicine, Cardiovascular Research Institute, UMDNJ — New Jersey Medical School, 185 South Orange Avenue, MSB G-609, Newark, New Jersey 07103-2714, USA. Phone: 973.972.8619; Fax: 973.972.7489; E-mail: sadoshju@umdnj.edu.

1. Matallanas D, Romano D, Hamilton G, Kolch W, O'Neill E. A Hippo in the ointment: MST signalling beyond the fly. *Cell Cycle*. 2008;7(7):879–884.
2. Yamamoto S, et al. Activation of Mst1 causes dilated cardiomyopathy by stimulating apoptosis without compensatory ventricular myocyte hypertrophy. *J Clin Invest*. 2003;111(10):1463–1474.
3. Odashima M, et al. Inhibition of endogenous Mst1 prevents apoptosis and cardiac dysfunction without affecting cardiac hypertrophy after myocardial infarction. *Circ Res*. 2007;100(9):1344–1352.
4. Matsui Y, et al. Lats2 is a negative regulator of myocyte size in the heart. *Circ Res*. 2008;103(11):1309–1318.
5. Vavvas D, Li X, Avruch J, Zhang XF. Identification of Nore1 as a potential Ras effector. *J Biol Chem*. 1998;273(10):5439–5442.
6. Dammann R, Li C, Yoon JH, Chin PL, Bates S, Pfeifer GP. Epigenetic inactivation of a RAS association domain family protein from the lung tumour suppressor locus 3p21.3. *Nat Genet*. 2000;25(3):315–319.
7. Zabarovsky ER, Lerman MI, Minna JD. Tumor suppressor genes on chromosome 3p involved in the pathogenesis of lung and other cancers. *Oncogene*. 2002;21(45):6915–6935.
8. Hesson LB, Cooper WN, Latif F. Evaluation of the 3p21.3 tumour-suppressor gene cluster. *Oncogene*. 2007;26(52):7283–7301.
9. Donninger H, Vos MD, Clark GJ. The RASSF1A tumor suppressor. *J Cell Sci*. 2007;120(pt 18):3163–3172.
10. van der Weyden L, Adams DJ. The Ras-association domain family (RASSF) members and their role in human tumourigenesis. *Biochim Biophys Acta*. 2007;1776(1):58–85.
11. Tommasi S, et al. Tumor susceptibility of Rassf1a knockout mice. *Cancer Res*. 2005;65(1):92–98.
12. van der Weyden L, et al. The RASSF1A isoform of RASSF1 promotes microtubule stability and suppresses tumorigenesis. *Mol Cell Biol*. 2005; 25(18):8356–8367.
13. Scheel H, Hofmann K. A novel interaction motif, SARAH, connects three classes of tumor suppressor. *Curr Biol*. 2003;13(23):R899–R900.
14. Avruch J, et al. Rassf family of tumor suppressor polypeptides. *J Biol Chem*. 2009;284(17):11001–11005.
15. Vos MD, Ellis CA, Bell A, Birrer MJ, Clark GJ. Ras uses the novel tumor suppressor RASSF1 as an effector to mediate apoptosis. *J Biol Chem*. 2000;275(46):35669–35672.
16. Ortiz-Vega S, et al. The putative tumor suppressor RASSF1A homodimerizes and heterodimerizes with the Ras-GTP binding protein Nore1. *Oncogene*. 2002;21(9):1381–1390.
17. Praskova M, Khoklatchev A, Ortiz-Vega S, Avruch J. Regulation of the MST1 kinase by autophosphorylation, by the growth inhibitory proteins, RASSF1 and NORE1, and by Ras. *Biochem J*. 2004; 381(pt 2):453–462.
18. Katagiri K, Imamura M, Kinashi T. Spatiotemporal regulation of the kinase Mst1 by binding protein RAPL is critical for lymphocyte polarity and adhesion. *Nat Immunol*. 2006;7(9):919–928.
19. Oh HJ, et al. Role of the tumor suppressor RASSF1A in Mst1-mediated apoptosis. *Cancer Res*. 2006;66(5):2562–2569.
20. Guo C, Tommasi S, Liu L, Yee JK, Dammann R, Pfeifer GP. RASSF1A is part of a complex similar to the Drosophila Hippo/Salvador/Lats tumor-suppressor network. *Curr Biol*. 2007;17(8):700–705.
21. Matallanas D, et al. RASSF1A elicits apoptosis through an MST2 pathway directing proapoptotic transcription by the p73 tumor suppressor protein. *Mol Cell*. 2007;27(6):962–975.
22. Polesello C, Huelsmann S, Brown NH, Tapon N. The Drosophila RASSF homolog antagonizes the hippo pathway. *Curr Biol*. 2006;16(24):2459–2465.
23. Oceandy D, et al. Tumor suppressor Ras-association domain family 1 isoform A is a novel regulator of cardiac hypertrophy. *Circulation*. 2009;120(7):607–616.
24. Freund C, et al. Requirement of nuclear factor-kappaB in angiotensin II- and isoproterenol-induced cardiac hypertrophy in vivo. *Circulation*. 2005; 111(18):2319–2325.
25. Ozes ON, Mayo LD, Gustin JA, Pfeffer SR, Pfeffer LM, Donner DB. NF-kappaB activation by tumour necrosis factor requires the Akt serine-threonine kinase. *Nature*. 1999;401(6748):82–85.
26. Romashkova JA, Makarov SS. NF-kappaB is a target of AKT in anti-apoptotic PDGF signalling. *Nature*. 1999;401(6748):86–90.
27. Brockman JA, et al. Coupling of a signal response domain in I kappa B alpha to multiple pathways for NF-kappa B activation. *Mol Cell Biol*. 1995; 15(5):2809–2818.
28. Radu M, Chernoff J. The DeMSTification of mammalian Ste20 kinases. *Curr Biol*. 2009;19(10):R421–R425.
29. Cheung WL, et al. Apoptotic phosphorylation of histone H2B is mediated by mammalian sterile twenty kinase. *Cell*. 2003;113(4):507–517.
30. Lehtinen MK, et al. A conserved MST-FOXO signaling pathway mediates oxidative-stress responses and extends life span. *Cell*. 2006;125(5):987–1001.
31. Chan EH, Nousiainen M, Chalamalasetty RB, Schafer A, Nigg EA, Sillje HH. The Ste20-like kinase Mst2 activates the human large tumor suppressor kinase Lats1. *Oncogene*. 2005;24(12):2076–2086.
32. Graves JD, et al. Caspase-mediated activation and induction of apoptosis by the mammalian Ste20-like kinase Mst1. *EMBO J*. 1998;17(8):2224–2234.
33. Zhou D, et al. The Nore1B/Mst1 complex restrains antigen receptor-induced proliferation of naive T cells. *Proc Natl Acad Sci U S A*. 2008;105(51):20321–20326.
34. Mann DL, Spinale FG. Activation of matrix metalloproteinases in the failing human heart: breaking the tie that binds. *Circulation*. 1998;98(17):1699–1702.
35. Goldsmith EC, et al. Organization of fibroblasts in the heart. *Dev Dyn*. 2004;230(4):787–794.
36. Yokoyama T, et al. Angiotensin II and mechanical stretch induce production of tumor necrosis factor in cardiac fibroblasts. *Am J Physiol*. 1999; 276(6 pt 2):H1968–H1976.
37. Harvey KF, Pfleger CM, Hariharan IK. The Drosophila Mst ortholog, hippo, restricts growth and cell proliferation and promotes apoptosis. *Cell*. 2003;114(4):457–467.
38. Wu S, Huang J, Dong J, Pan D. hippo encodes a Ste-20 family protein kinase that restricts cell proliferation and promotes apoptosis in conjunction with salvador and warts. *Cell*. 2003;114(4):445–456.
39. Song H, et al. Mammalian Mst1 and Mst2 kinases play essential roles in organ size control and tumor suppression. *Proc Natl Acad Sci U S A*. 2010; 107(4):1431–1436.
40. Lu L, et al. Hippo signaling is a potent in vivo growth and tumor suppressor pathway in the mammalian liver. *Proc Natl Acad Sci U S A*. 2010; 107(4):1437–1442.
41. Yokoyama T, Nakano M, Bednarczyk JL, McIntyre BW, Entman M, Mann DL. Tumor necrosis factor-alpha provokes a hypertrophic growth response in adult cardiac myocytes. *Circulation*. 1997; 95(5):1247–1252.
42. Sadoshima J, Izumo S. Molecular characterization of angiotensin II-induced hypertrophy of cardiac myocytes and hyperplasia of cardiac fibroblasts: a critical role of the AT1 receptor subtype. *Circ Res*. 1993;73(3):413–423.
43. Sadoshima J, et al. The MEKK1-JNK pathway plays a protective role in pressure overload, but does not mediate cardiac hypertrophy. *J Clin Invest*. 2002;110(2):271–279.